

# Critical dynamics of superconducting BSCCO films

K. D. Osborn\* and D. J. Van Harlingen, Vivek Aji, Nigel Goldenfeld, S. Oh and J. N. Eckstein

Department of Physics,  
University of Illinois at Urbana-Champaign  
1110 West Green Street  
Urbana, IL, 61801-3080

(Dated: February 7, 2020)

We report on a systematic investigation of the critical fluctuations in the complex conductivity of epitaxially-grown  $\text{Bi}_2\text{Sr}_2\text{CaCu}_2\text{O}_{8+\delta}$  films for  $T \lesssim T_c$  using a two-coil inductive technique at zero applied field. We observe the static 3D-XY critical exponent in the superfluid density near  $T_c$ . Linear scaling analysis close to the critical temperature yields a dynamic critical exponent of  $z \approx 2.0$  for small drive currents, but non-linear effects are seen to be important. At  $T_c$ , a non-linear scaling analysis also yields a 3D dynamic exponent of  $z = 2.0 \pm 0.1$ .

PACS numbers: 74.40.+k, 74.25.Nf, 74.72.Hs, 74.76.Bz

## I. INTRODUCTION

Direct observation of the scaling properties of the superconducting transition has at last become feasible due to the discovery of the cuprate superconductors. Microwave measurements in ultrapure single crystal  $\text{YBa}_2\text{Cu}_3\text{O}_{7-x}$  (YBCO) have provided strong evidence that for accessible temperature ranges, the effective static universality class is the three dimensional XY model (3D-XY)<sup>1</sup>, where the penetration depth displayed scaling over three decades in reduced temperature. Measurements on thin films have yielded varying results: microwave measurements report  $\nu = 1.2$ <sup>2</sup>, contactless ac conductivity measurements yield  $\nu = 1.7$  at frequencies up to 2 GHz<sup>3</sup> and dc conductivity in finite magnetic fields give  $\nu = 0.9 - 1.0$ <sup>4</sup>. While none of these agree with the 3D-XY scaling behavior, it is widely believed that the results on pure single crystals is indicative of the intrinsic critical fluctuations of the superconducting transition.

Transport measurements have probed the dynamics of the critical fluctuations, which are characterized by the value of the dynamic critical exponent  $z$  describing how the relaxation time  $\tau$  scales with the correlation length  $\xi$ :  $\tau \sim \xi^z$ . However for YBCO, experiments have not yielded a consistent picture. For example, longitudinal dc-resistivity measurements yield  $z = 1.5 \pm 0.1$ <sup>5</sup> in magnetic fields up to 6 T, while microwave conductivity measurements are consistent with  $z = 2.3 - 3.0$ <sup>2</sup>. Still larger values for the dynamic exponent of  $z = 5.6$ <sup>3</sup> and  $z = 9, 10$ <sup>4</sup> reminiscent of glassy dynamics have also been seen in thin films. These large values of  $z$  strongly suggest that disorder plays a dominant role in these thin films, and this may explain why their observed static critical behavior differs from that of the best single crystals.

Critical fluctuation results on  $\text{Bi}_2\text{Sr}_2\text{CaCu}_2\text{O}_{8+\delta}$  (BSCCO) are even more dissimilar. In previous work on BSCCO crystals a non-linear transport study found 2D critical behavior with an anomalous dynamic exponent of  $z \approx 5.6$  and no crossover to 3D behavior<sup>6</sup>. The 3D universal phase angle of the complex conductivity deduced from the magnetic susceptibility of BSCCO yields

an even larger value of  $z$ <sup>7</sup>. However, the complex conductivity of underdoped BSCCO measured at terahertz frequencies agrees with a Kosterlitz-Thouless-Berezinskii (KTB) model with diffusive dynamics<sup>8,9</sup>. Only dc fluctuation conductivity measurements in BSCCO find relaxational dynamics,  $z \approx 2.0$ , *assuming* a 3D-XY static exponent,  $\nu \approx 2/3$ <sup>10</sup>, in agreement with recent theoretical work that predicts that  $z \approx 2.0$  in 3D<sup>11</sup>. These results indicate the lack of consensus on the true nature of the dynamic fluctuations representative of the superconducting transition, which is the primary motivation of the present investigation. While a large value of the dynamic exponent ( $z > 2$ ) can be understood as disorder effects, only the presence of a previously undetected collective mode coupled to the superfluid density would lead to  $z \approx 1.5$  in 3D, just as occurs in superfluid He<sup>4</sup><sup>12</sup>.

In this paper we provide results on the critical fluctuations in high quality epitaxially-grown BSCCO films. We have measured the ab-plane complex conductivity with a two-coil inductive technique at zero applied magnetic field ( $H = 0$ ), described in Section II. Our measurements, presented in section III, indicate that the critical fluctuations in BSCCO films are consistent with the 3D-XY critical fluctuation model, rather than a KTB transition within the layers. This contrasts with previous studies using this technique on YBCO, which report KTB critical<sup>13</sup> and mean-field<sup>14</sup> fluctuations. In section IV, we estimate the temperature intervals in which possible crossovers to two dimensional fluctuations can occur, due either to decoupling of the bilayers or to the thin film behaving as a two-dimensional system due to a large  $c$ -axis correlation length. We find that our measurements should indeed be well-described by 3D-XY critical fluctuations. In section V, we provide a crossover analysis of the approach to the critical point, and examine the approach to a universal phase angle. In particular, we predict the qualitative form of the variations with temperature and frequency, in agreement with our measurements, but which contrast with earlier results in the literature which report very different values of the static and dynamic critical exponents than those reported here. Anal-

ysis of the phase angle of the film response is presented in section VI, using linear response theory in the critical region, yields a dynamic exponent of  $z = 2.0$ . However, the breakdown of linear response theory becomes important near the transition temperature  $T_c$  and the analysis is complicated by the need to extract the superfluid density from the measured mutual inductance by an approximate inversion technique. Our analysis shows that the determination of  $z$  purely from linear response theory is contaminated by non-linear effects, and at probe currents that are too large the effective value of  $z$  inferred can be as low as 1.5. To circumvent this problem we derive in section VII a non-linear scaling law obeyed by the raw measured mutual inductance at  $T_c$  (i.e. without the need for a data inversion) and extract the dynamic exponent directly from the mutual inductance. In agreement with the linear response analysis, we again obtain  $z \approx 2.0$ . Section VIII summarizes our conclusions.

## II. EXPERIMENTAL SETUP

We have measured several high quality oxygen-doped BSCCO films, grown by molecular-beam-epitaxy on  $\text{SrTiO}_3$  substrates and analyzed in-situ by RHEED<sup>15</sup>. The BSCCO films are nominally oriented along the  $c$ -axis, with unit cell thickness of  $d = 15.4 \text{ \AA}$ . Films A, B, and C have  $n = 21, 40$  and  $60$  unit cells respectively and are grown on  $10$  and  $14$  mm square substrates. Film A is overdoped, while film B and C are slightly overdoped and underdoped, respectively.

To obtain the ab-plane complex conductivity, we employ a two-coil inductive technique. The mutual inductance of two coaxial coils is measured with a film placed in between and normal to the axis of the coils. An ac current is applied through the drive coil; a second coil, attached to a large input impedance lock-in amplifier, measures the fields produced by the drive coil and the screening currents in the film. The coils have 135 turns and an average radius of 1.5 mm. The drive coil is placed 0.35 mm above the film so that at a current of  $I = 50 \mu\text{A}$  rms the applied ac magnetic field is  $< 0.1$  Gauss normal to the film. Measurements are performed in a  $\text{He}^4$  continuous-flow dewar, which allows the temperature of the film to be controlled without significant heating from the drive coil. The sample temperature is monitored by a Si diode attached to the back side of the substrate.

## III. STATIC CRITICAL BEHAVIOR

The complex conductivity  $\sigma = \sigma_1 - i\sigma_2$  of each film is calculated from the mutual inductance using the exact analytical expression for an infinite diameter film<sup>16</sup> and a numerical inversion technique similar to that of Fiory *et al.*<sup>17</sup>. The method of Turneaure *et al.*<sup>18</sup> is employed to correct for film diameter effects prior to calculating the in-plane complex conductivity. The measured

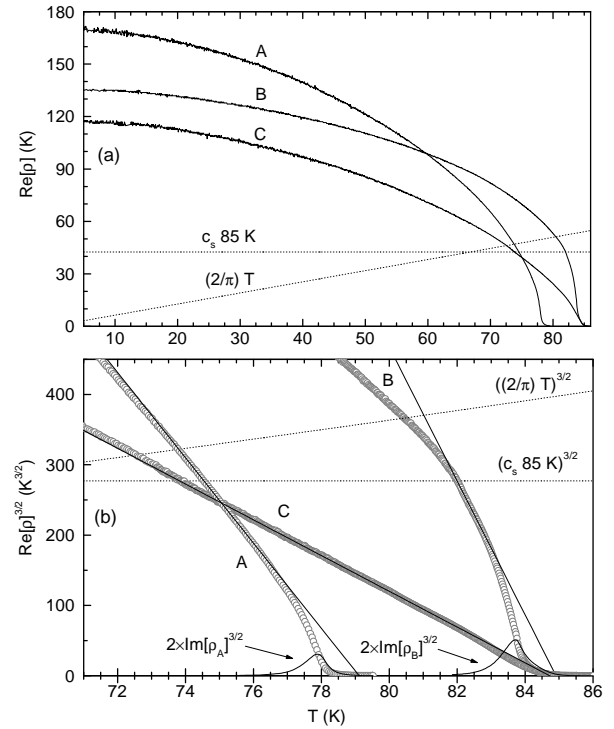


FIG. 1:  $Re[\rho]$  (panel a) and  $Re[\rho]^{3/2}$  (panel b), as a function of temperature for films A through C.  $\rho = (c_s 85 \text{ K})$  is the predicted crossover to 3D-XY critical behavior and  $\rho = (2/\pi)T$  is the KTB critical superfluid density for an isolated bilayer.

penetration depth  $\lambda_{ab} = (\mu_0 \omega \sigma_2)^{-1/2}$ , is independent of the measurement frequency from  $f = 10 - 100$  kHz below the transition temperature, where the dissipation is small ( $\sigma_1 \ll \sigma_2$ ). To analyze the critical fluctuations, we study the complex superfluid density per CuO bilayer,  $\rho = i\sigma\omega d\Phi_0^2/(4\pi^2 k_B)$ , where  $\Phi_0$  is the superconducting flux quantum<sup>19</sup>. The real part of this quantity,  $Re[\rho]$  has units of temperature and sets the energy scale for critical fluctuations. In Fig. 1(a)  $Re[\rho]$  is plotted for films A through C, obtained at  $f = 80$  kHz and  $I = 40 \mu\text{A}$ . At 5 K, films A, B, and C, have penetration depths of 235, 265, and 285 nm, respectively. The low temperature doping and temperature dependence will be discussed elsewhere.

The mean field behavior, expected at low temperatures, crosses over to the 3D-XY behavior as the critical temperature is approached from below. In layered systems, the 3D-XY behavior is exhibited once the  $c$ -axis correlation length exceeds the interlayer spacing,  $d$ ; i.e. when  $\rho(T) = c_s T_c$ , where  $c_s \approx 0.5$  and  $\rho = Re[\rho]^1$ . In Fig. 1(b), the data from Fig. 1(a), are plotted as  $Re[\rho]^{3/2}$  near the critical regime. Also shown in Figs. 1(a) and 1(b) is the corresponding power of  $c_s T_c$  to locate the onset of 3D-XY behavior. The static 3D-XY model gives  $\rho \sim \xi^{-1} \sim |T - T_c|^\nu$ , where  $\nu \approx 2/3$ . We observe that  $Re[\rho]^{3/2}$  varies linearly in temperature for  $\rho(T) \lesssim c_s T_c$  indicating a 3D-XY, rather than mean-field ( $\rho \sim |T - T_c|$ ), behavior. At our measurement current

(40  $\mu$ A), we observed an absence of frequency dependence, below the dissipation peak, over the temperature range of the fit. In film C the linear regime is as large as 7 K below 82 K. The linear fits extrapolate to estimates of  $T_c = 79.1$  K, 84.9 K and 84.7 K for films A, B and C respectively.

Although our static scaling analysis is analyzed at temperatures and a drive current with no frequency dependence, at higher temperatures we observe current as well as frequency dependence. This is apparent in Fig. 2, where larger currents are used on film B with 40 layers. Film C, with 60 layers, exhibited a weaker dependence over the same frequencies and currents. Since the superfluid density depends on frequency and current at higher temperatures, the superfluid density scales as  $\rho \sim \xi^{2-D} f(\omega \xi^z, E \xi^{1+z})$ , where  $E$  is the amplitude of the electric field. Only in the critical regime where the data are independent of both the frequency and the electric field can one expect to see the linear response scaling behavior and extract the exponent  $\nu$ . At higher temperatures where we observe non-linear behavior as well as frequency dependence, the data are still consistent with the 3D-XY fluctuations, and we can extract  $z$ . In section VI we analyze the phase angle in terms of linear response

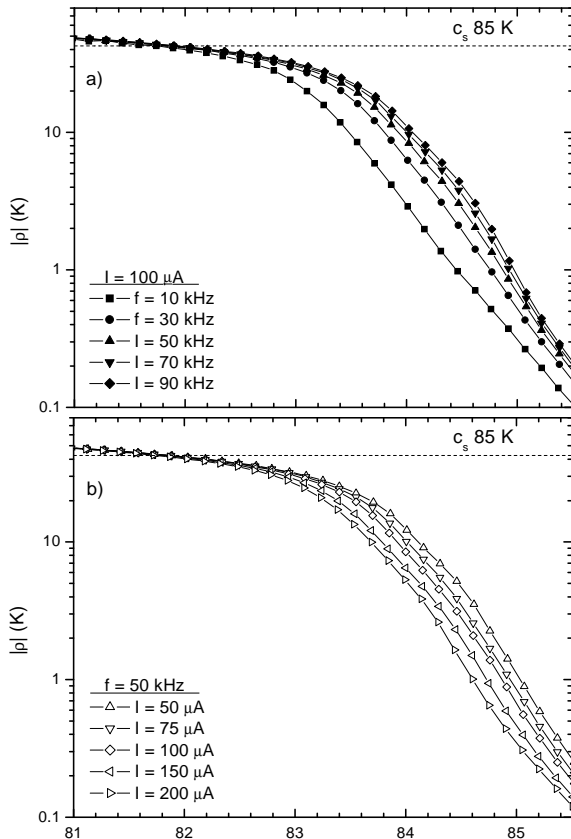


FIG. 2:  $|\rho|$  in film B taken at a series of frequencies (panel a) and drive currents (panel b).

#### IV. DIMENSIONALITY OF THE STATIC FLUCTUATIONS

In Figs. 1(a) and 1(b) a power of  $2T/\pi$  is shown to locate where we would expect the KTB transition for a noninteracting bilayer,  $\rho = 2T/\pi^{20}$ . We observe no drop in the superfluid density at this temperature in our films. The films instead exhibit three dimensional behavior with coupling among the bilayers, precluding a KTB transition in the bilayers. At higher temperatures we do observe a drop in the superfluid density from the static scaling value which may be interpreted as a crossover to two dimensional behavior. We do not believe this to be the case in our films since the drop is observed to be current as well as frequency dependent (see Fig. 2). Notice that the superfluid density does drop more rapidly than expected from the 3DXY model as the frequency is decreased for a given drive current, but does so more slowly as the current is decreased at fixed frequency. While the former might lead one to conclude that 3DXY behavior is not valid in the static limit, the latter would imply the opposite. More accurate measurements are needed at low frequency and currents to establish unambiguously the true nature of the static limit. Nevertheless the trend with decreasing current, coupled with the phase angle dependence discussed in the next section, is consistent with 3DXY behavior. Another putative crossover to 2D behavior is expected when  $\xi_c$  becomes as large as the film thickness,  $h$ . 3D-XY scaling implies that this occurs at a temperature,  $T^*$ , which is 0.05 K, 0.01 K and 0.02 K below the transition temperature for films A, B and C respectively. This implies that the region of pure 2D fluctuations is too small to be resolved in our data and therefore we expect 3D fluctuations to dominate.

#### V. CROSSOVER PHENOMENA IN THE LINEAR PHASE ANGLE NEAR $T_c$

Since the experiments are performed at finite frequency, it is important to consider whether or not the correct asymptotic behavior is being probed and what conclusions can be drawn from the observed behavior. We begin with the superfluid density, within linear response, written as

$$\rho = (t^{-\nu})^{2-D} f_1(\omega t^{-\nu z}) \quad (1)$$

where  $t = |T - T_c|/T_c$  and  $f_1$  is a scaling function. In the limit of  $t \rightarrow 0$  ( $T \rightarrow T_c$ ), the  $t$ -dependence must cancel out of the expression for  $\rho$ , which implies that the asymptotic behavior of the scaling function  $f_1(x) \sim x^\theta$  as  $x \rightarrow \infty$  where  $\theta = (2 - D)/z$ . For  $t \neq 0$ , we can write

$$\rho = (i\omega)^{(D-2)/z} f_2(t\omega^{-1/\nu z}) \quad (2)$$

where the scaling function  $f_2(y) = \text{const}$  as  $y \rightarrow 0$ . We now ask what behavior we should observe as  $\omega \rightarrow 0$  for

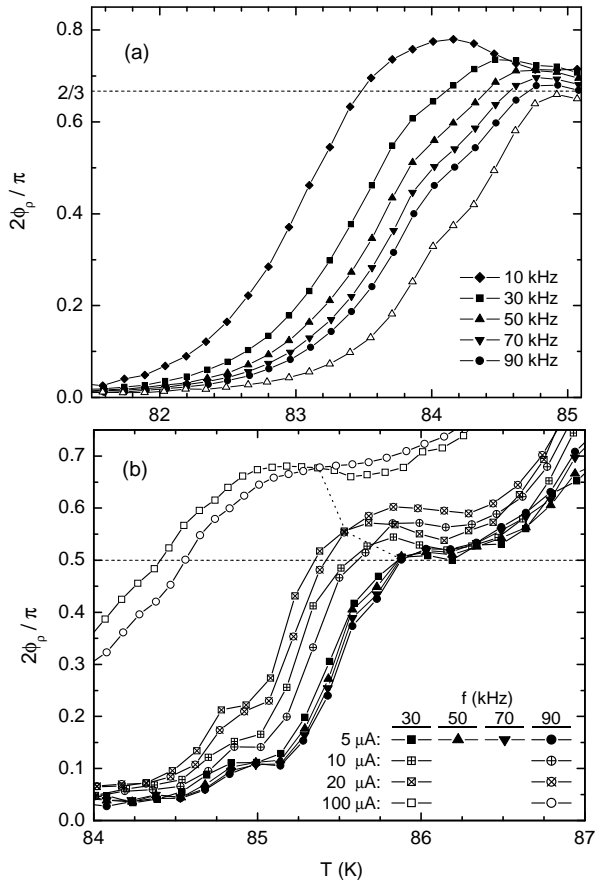


FIG. 3: Normalized phase angle,  $2\phi_\rho/\pi$ , of the superfluid density extracted from linear response theory. Panel a:  $2\phi_\rho/\pi$  in film B taken at  $I = 100\mu\text{A}$  (filled symbols) at a series of frequencies and  $I = 50\mu\text{A}$  for  $f = 50\text{kHz}$  (unfilled triangles). Panel b:  $2\phi_\rho/\pi$  in film C for a given table of frequencies and drive currents.

$t \neq 0$ . For  $\omega \rightarrow 0$  at  $t = 0$ , we should see the critical point behavior. For  $t/\omega^{1/\nu z} \ll 1$  we are probing the  $y \sim 0$  regime of the scaling function  $f_2(y)$  and expect to see asymptotic scaling behavior. If  $t/\omega^{1/\nu z} \gg 1$  we are probing the  $y \rightarrow \infty$  regime of the argument of  $f_2$  and do not expect to see the scaling behavior. Thus at a finite  $t_0$ , for  $\omega \gg t_0^{4/3}$  we would observe critical behavior while for  $\omega \ll t_0^{4/3}$  we would not. We have used the critical exponents  $\nu = 2/3$  and  $z = 2$  for specificity, but the argument does not rely on these precise values. Note that, as is generally the case with crossover, the behavior of the superfluid density away from the critical point at finite frequencies is not universal except in the large frequency limit - a result that is sometimes found to be surprising, but which follows from a generic crossover analysis of relevant variables<sup>21</sup>. This predicted low frequency behavior is consistent with our data where we observe the critical phase angle in Fig. 3(b) and yet we do not observe scaling below  $T_c$ . More importantly, this is also consistent with the non-linear scaling observed at

$T_c$  in Section VII. Away from  $T_c$  an asymptotic scaling regime is demonstrated in the microwave measurements of Booth *et al*<sup>2</sup>.

## VI. DYNAMIC CRITICAL BEHAVIOR AND THE BREAKDOWN OF LINEAR RESPONSE THEORY

Next we study the phase of  $\rho$ ,  $\phi_\rho$ , close to the transition temperature. The frequency dependence of  $2\phi_\rho/\pi$  for film B measured at  $I = 100\mu\text{A}$  is shown in Fig. 3(a). Within linear response theory, the phase angle is independent of frequency at the critical temperature and is given by  $\phi_\rho(T_c) = \pi/(2z)$  in three dimensions, where  $z$  is the dynamic critical exponent<sup>22</sup>. In Fig. 3(a) we notice that the curves for different frequencies seem to approach a phase angle consistent with a dynamic exponent of  $z \approx 1.5$  and  $T_c = 84.9\text{ K}$ . When repeated at a smaller value of the current,  $I = 50\mu\text{A}$ ,  $\phi_\rho(T_c)$  is smaller, as shown. Since the constant phase angle is a result from linear response theory, the estimate of the dynamic exponent from the data is expected to be more accurate at smaller currents.

This is indeed seen in the current dependence of the phase angle at different frequencies for film C. In Fig. 3(b),  $2\phi_\rho/\pi$  is shown for a set of frequencies and currents. As the current is lowered, the frequency independent phase angle shifts to lower values. At  $20\mu\text{A}$ ,  $10\mu\text{A}$  and  $5\mu\text{A}$ , this phase angle is  $0.57\pi/2$ ,  $0.54\pi/2$  and  $0.51\pi/2$  respectively. This suggests that the result of  $z \approx 1.5$  from film B is an artifact of the large current used in the measurement. With this analysis, the thickest film (C) exhibits a critical phase angle, the film with intermediate thickness (B) provides evidence for similar behavior, but the thinnest film did not show a critical phase angle. Due to the crossover phenomena discussed in the previous section, the behavior of the phase angle away from  $T_c$  is not universal at low frequencies, but we can still infer the dynamic critical exponent from the critical phase angle at  $T_c$  which is indeed universal.

Both the phase angle and the superfluid density is found to be dependent on the drive current near  $T_c$ . In the limit of smaller currents, the frequency independent critical phase angle does indeed yield a dynamic exponent of  $z \approx 2.0$ . This is a result consistent with the presence of 3D fluctuations. This is also consistent with the behavior of the superfluid density with decreasing current, at fixed frequency, where it is seen to approach the asymptotic static scaling law. Furthermore, the smooth evolution of the phase angle, suggests that the crossover to the two dimensional regime near  $T^*$ , is not resolved in our experiment. Nevertheless, the fact that nonlinear scaling and dimensional crossover is expected close to  $T_c$ , we now proceed to analyze the nonlinear response, to get a more accurate determination of the dynamic exponent.

## VII. NONLINEAR SCALING AT THE SUPERCONDUCTING TRANSITION

The field equation governing the vector potential,  $\vec{A}$ , is

$$\nabla^2 \vec{A}/\mu_0 = -\vec{J}_d - h\delta(z)\sigma\vec{E} \quad (3)$$

where  $\vec{J}_d$  is the current density in the drive coil,  $\sigma$  is the conductivity of the superconducting film, and  $\vec{E}$  is the electric field. For the geometry of the setup,

$$\vec{J}_d = I_d\delta(r - r_c)\delta(z - z_c)\hat{\phi} \quad (4)$$

in cylindrical coordinates, where  $I_d$  is the drive current,  $r_c$  is the radius of the drive coil and  $z_c$  is the distance from the film to the drive coil<sup>16</sup>. For an anisotropic system, in the critical regime, the superfluid density,  $\rho$ , scales as,

$$\rho \sim i\omega\sigma \sim \xi_{ab}^{3-D}\xi_c^{-1}f(i\omega\xi_{ab}^z, E\xi_{ab}^{1+z}) \quad (5)$$

where  $\xi_{ab}$  and  $\xi_c$  are the correlation lengths parallel and perpendicular to the CuO bilayers, and  $f$  is a scaling function. We can rewrite the field equation as

$$\begin{aligned} \nabla^2 A = & -\mu_0 I_d\delta(r - r_c)\delta(z - z_c) \\ & - h\xi_{ab}^{3-D}\xi_c^{-1}f(\omega\xi_{ab}^z, A\xi_{ab})A\delta(z) \end{aligned} \quad (6)$$

where we have used the scaling form for the complex conductivity. Since the scaling function is written in terms of dimensionless variables we can non dimensionalise the equation by recasting it in terms of  $A\xi_{ab}$ ,  $\omega\xi_{ab}^z$ ,  $r/h$  and  $I_d\xi_{ab}$ . The solution then takes the form,

$$Ai\omega\xi_{ab}^{1+z} = G(i\omega\xi_{ab}^z, i\omega\xi_{ab}^{1+z}I_d, h^2\xi_{ab}^{3-D}\xi_c^{-1}\Lambda^{-1}, r/h) \quad (7)$$

where  $G$  is a function that can be determined by solving the full non-linear field equation and  $\Lambda$  is the thermal length given by  $\Phi_0^2/(4\pi\mu_0 k_B T)$ . So far all we have done is to use the scaling form for the superfluid density and looked for a generic solution of a differential equation by identifying all the nondimensional variables. For a given geometry of the experiment the right hand side of Eqn. 7 is a function of three variables. One can further simplify the expression if we realise that there exists a regime  $|T - T_c| < T^*$  where we are governed by the limit where  $\xi_c = h$ . This allows us to eliminate one of the three terms as follows. Close to  $T_c$ , using the 3D-XY behavior of the correlation length and the definition of  $T^*$ , we can rewrite  $h^2\xi_{ab}^{3-D}/\xi_c$  as,

$$h^2\xi_{ab}^{3-D}/\xi_c = h|1 + (T - T^*)/(T^* - T_c)|^\nu \quad (8)$$

For a temperature range  $|T - T^*| \ll |T^* - T_c|$ ,  $h^2/\xi_c \approx h$ . Thus, for temperatures within  $0.05K$ ,  $0.02K$ , and  $0.01K$  of  $T^*$  for films a, b, and c respectively, this approximation is valid, and the field in Eqn. 7 is a function of only two variables for a given geometry. Thus one can now perform the standard data collapse at  $T_c$  of the

measured mutual inductance to obtain the dynamic exponent. In this regime we can eliminate  $\xi_{ab}$  from Eqn.7 so that

$$A = \omega^{1/z}\tilde{G}(I_d\omega^{-1/z}, h\Lambda^{-1}, r/h) \quad (9)$$

The mutual inductance,  $M$ , is related to the vector potential at the pick up coil and scales as

$$M \sim A\omega^{-1/z} \sim \tilde{G}(I_d i\omega^{-1/z}) \quad (10)$$

Within the resolution of our data, any data collapse observed is a 3D phenomena starting to crossover to the asymptotic 2D scaling. The reason for this is that the solution (Eqn. 7) depends on a number of variables, but sufficiently close to  $T_c$  there exists a regime wherein the mutual inductance is only a function of one scaling variable. If we do not observe any data collapse we would conclude that we are never in the regime where the approximation  $h^2/\xi_c \approx h$  is valid. It is indeed true that the elimination of the dependence of  $\xi_{ab}$  in Eqn. 7 is possible only at  $T_c$  and need not hold in the entire regime where the crossover occurs. It is tempting to interpret the experimental results in terms of a two dimensional system. Our data on the other hand are unable to resolve the crossover regime, and yet do exhibit data collapse (see Fig 4). This suggests that the temperature at which we observe data collapse lies in the crossover regime, but is not necessarily the true  $T_c$ . From our analysis we conclude that the  $T_c$  is within  $0.02$  K of the temperature at which we observe data collapse for film B and C. We now look for data collapse of our data measured by varying frequency, current and temperature. Notice that the value of the exponent  $\nu$  is required only to establish the regime of validity of the approximation and is not necessary to extract the dynamic exponent from data collapse at  $T_c$ .

For the scaling analysis at  $T_c$ , the mutual inductance at fixed frequency,  $M_f$ , was compared to the mutual inductance at fixed current,  $M_I$ . Values of  $M_f$  ( $M_I$ ), were measured at  $12.5 \mu\text{A}$  ( $10 \text{ kHz}$ ) intervals for a set of fixed temperatures. Then values of  $|M_f|$  were compared with values of  $|M_I|$  taken at the same temperature by fitting the raw data of  $|M_f|$  to a polynomial and selecting points with the values of  $I\omega^{-1/z}$  equivalent to those of  $|M_I|$ . In Fig. 4(a)  $|M_f|$  and  $|M_I|$  for film B are plotted versus  $I\omega^{-1/2}$  for a series of temperatures. The best data collapse of the curves appear at  $z = 2.0$  and  $T = 85.22$  K. The error in the scaling,  $\Delta_M$ , is shown in Fig. 4(b) for different temperatures and values of  $z$ . This is obtained from  $\Delta_M^2 = \sum (|M_f| - |M_I|)^2$ , where the sum runs over the 10 values of  $I\omega^{-1/z}$  measured for  $|M_I|$ . The lowest error value indicates  $z = 2.0 \pm 0.1$  and  $T = 85.2 \pm 0.1$  K. A similar analysis for the film C yields  $z = 1.8 \pm 0.2$  and  $T = 85.9 \pm 0.2$  K, which is also consistent with  $z = 2.0 \pm 0.1$ . The transition temperature of film B is  $T_c = 85.2 \pm 0.1$  K, while for film C it is  $T_c = 85.9 \pm 0.2$  K. These values of  $T_c$  are close to those obtained with the phase angle measurements.

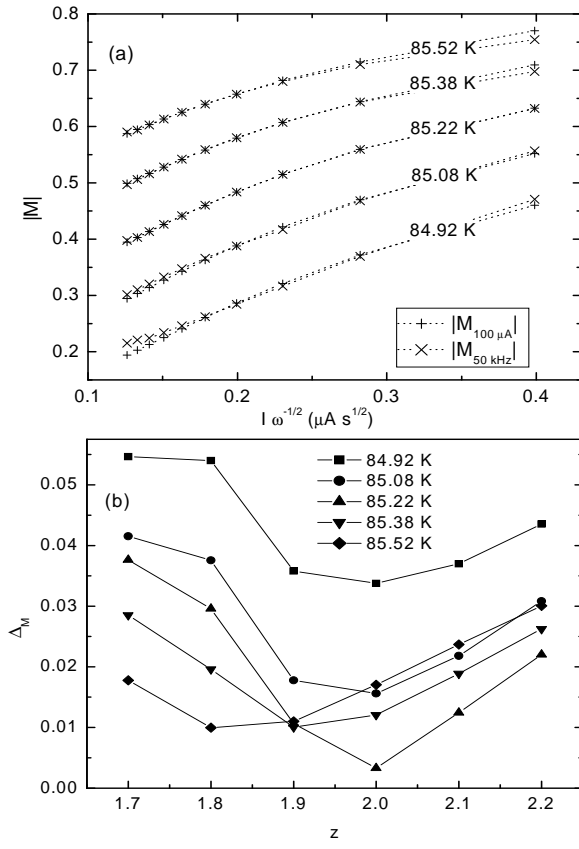


FIG. 4: Panel (a):  $|M|$  measured at  $I = 100\mu\text{A}$  and  $f = 50$  kHz versus the scaling variable  $I\omega^{-1/2}$ . Panel (b): Scaling error at different temperatures versus  $z$ .

In Fig. 4(b), the evolution of the error for a fixed trial

$z$ , also suggests that the dynamic exponent observed is indeed due to  $3D$  fluctuations. Notice that as the temperature is increased for  $z = 2.0$ , the error decreases, approaching the best fit (i.e. data collapse), and then increases again. Within the resolution of the data, we never observe any change to the  $2D$  regime. In other words, the approximation that allowed us to look for the data collapse, is indeed supported by the behavior of the mutual inductance.

## VIII. CONCLUSIONS

The superfluid density in BSCCO films with different thicknesses has been measured and shown to be *consistent* with the predictions of the  $3D$ -XY model. The dynamic scaling exponent has been obtained by performing both a linear and non-linear scaling analysis. While the linear scaling analysis did yield a  $3D$  dynamic exponent of  $z \approx 2.0$ , non-linear effects needed to be studied to get an accurate determination. This is evident from the current dependence of the critical phase angle of the superfluid density. A  $3D$  non-linear scaling analysis also yields a dynamic exponent of  $z = 2.0 \pm 0.1$ .

## Acknowledgments

We thank H. Westfahl and D. Sheehy for many helpful discussions. This work was partially supported by the Department of Energy under grant number DEFG02-96ER45439 and the National Science Foundation under grant number NSF-DMR-99-70690.

- \* Present address: National Institute of Standards and Technology, Boulder, CO, 80305
- <sup>1</sup> S. Kamal, D.A. Bonn, N. Goldenfeld, P.J. Hirshfeld, R. Liang, and W.N. Hardy, Phys. Rev. Lett. **73**, 1845 (1994). S. Kamal, R. Liang, A. Hosseini, D.A. Bonn, and W.N. Hardy, Phys. Rev. B **58**, R 8933 (1998).
- <sup>2</sup> J.C. Booth, D.H. Wu, S.B. Qadri, E.F. Skelton, M.S. Osofsky, A. Pique, and S.M. Anlage, Phys. Rev. Lett. **77**, 4438 (1996).
- <sup>3</sup> G. Nakielsky, D. Gorlitz, Chr. Stodte, M. Welters, A. Kramer and J. Koetzler, Phys. Rev B **55** 6077 (1997).
- <sup>4</sup> J.M. Roberts, B. Brown, B.A. Hermann and J. Tate, Phys. Rev. B **49**, 6890 (1994).
- <sup>5</sup> J.T. Kim, N. Goldenfeld, J. Giapintzakis and D.M. Ginsberg, Phys. Rev. B **56**, 118 (1997).
- <sup>6</sup> S.M. Ammirata, M. Friesen, S.W. Pierson, L.A. Gorham, J.C. Hunnicutt, M.L. Trawick and C.D. Keener, Physics C **313**, 225 (1999). S.W. Pierson, M. Friesen, S.M. Ammirata, J.C. Hunnicutt and L.A. Gorham, Phys. Rev. B. **60**, 1309 (1999).
- <sup>7</sup> J. Kotzler and M. Kaufmann, Phys. Rev. B **56**, 13734 (1997).

- <sup>8</sup> J. Corson, R. Mallozzi, J. Orenstein, J.N. Eckstein, and I. Bozovic, Nature **398**, 221 (1999).
- <sup>9</sup> P. Minnhagen, Rev. Mod. Phys. **59**, 1001 (1987).
- <sup>10</sup> S.H. Han, Y. Eltsev and O. Rapp, Jour. Low. Temp. Phys. **117** 1259 (1999). S.H. Han, Y. Eltsev and O. Rapp, Phys. Rev. B. **61**, 11776 (2000).
- <sup>11</sup> V. Aji and N.D. Goldenfeld, Phys. Rev. Lett **87**, 197003 (2001).
- <sup>12</sup> P.C. Hohenberg and B.I. Halperin, Rev. Mod. Phys. **49**, 435 (1977).
- <sup>13</sup> A.T. Fiory, A.F. Hebard, P.M. Mankiewich and R.E. Howard, Phys. Rev. Lett. **61** 1419 (1988).
- <sup>14</sup> Z.H. Lin, G.C. Spalding, A.M. Goldman, B.F. Bayman, and O.T. Valls, Europhys. Lett. **32**, 573 (1995). K.M. Paget, B.R. Boyce, and T.R. Lemberger, Phys. Rev. B **59**, 6545 (1999).
- <sup>15</sup> J.N. Eckstein, I. Bozovic, K.E. von Dessonneck, D.G. Schlom, J.S. Harris Jr., and S. M. Baumann Appl. Phys. Lett. **57**, 931 (1990).
- <sup>16</sup> J.R. Clem and M.W. Coffey, Phys. Rev. B **46**, 14662 (1992).
- <sup>17</sup> A.T. Fiory, A.F. Hebard, P.M. Mankiewich, and R.E.

<sup>18</sup> Howard, Appl. Phys. Lett. **52**, 2165 (1988).

<sup>18</sup> S.J. Turneaure, E.R. Ulm, and T.R. Lemberger, J. Appl. Phys. **79**, 4221 (1996). S.J. Turneaure, A.A. Pesetski, T.R. Lemberger, Jour. Appl. Phys. **83**, 4334 (1998).

<sup>19</sup> D.S. Fisher, M.P.A. Fisher and D.A. Huse, Phys. Rev. B **43** 130 (1990).

<sup>20</sup> M.R. Beasley, J.E. Mooij and T.P. Orlando, Phys. Rev. Lett. **42**, 1165 (1979).

<sup>21</sup> N. Goldenfeld, *Lectures on Phase Transitions and the Renormalization Group* (Addison-Wesley, Reading, Mass., 1992), p. 271.

<sup>22</sup> A.T. Dorsey, Phys. Rev. B **43**, 7575 (1991).